DOI: 10.3901/CJME.2013.01.001, available online at www.springerlink.com; www.cjmenet.com; www.cjmenet.com.cn

Driving and Braking Control of PM Synchronous Motor Based on Low-resolution Hall Sensor for Battery Electric Vehicle

GU Jing, OUYANG Minggao*, LI Jianqiu, LU Dongbin, FANG Chuan, and MA Yan

State Key Laboratory of Automotive Safety and Energy, Tsinghua University, Beijing 100084, China

Received November 7, 2011; revised July 26, 2012; accepted October 11, 2012

Abstract: Resolvers are normally employed for rotor positioning in motors for electric vehicles, but resolvers are expensive and vulnerable to vibrations. Hall sensors have the advantages of low cost and high reliability, but the positioning accuracy is low. Motors with Hall sensors are typically controlled by six-step commutation algorithm, which brings high torque ripple. This paper studies the high-performance driving and braking control of the in-wheel permanent magnetic synchronous motor (PMSM) based on low-resolution Hall sensors. Field oriented control (FOC) based on Hall-effect sensors is developed to reduce the torque ripple. The positioning accuracy of the Hall sensors is improved by interpolation between two consecutive Hall signals using the estimated motor speed. The position error from the misalignment of the Hall sensors is compensated by the precise calibration of Hall transition timing. The braking control algorithms based on six-step commutation and FOC are studied. Two variants of the six-step commutation braking control, namely, half-bridge commutation and full-bridge commutation, are discussed and compared, which shows that the full-bridge commutation could better explore the potential of the back electro-motive forces (EMF), thus can deliver higher efficiency and smaller current ripple. The FOC braking is analyzed with the phasor diagrams. At a given motor speed, the motor turns from the regenerative braking mode into the plug braking mode if the braking torque exceeds a certain limit, which is proportional to the motor speed. Tests in the dynamometer show that a smooth control could be realized by FOC driving control and the highest efficiency and the smallest current ripple could be achieved by FOC braking control, compared to six-step commutation braking control. Therefore, FOC braking is selected as the braking control algorithm for electric vehicles. The proposed research ensures a good motor control performance while maintaining low cost and high reliability.

Key words: battery electric vehicle, field oriented control, low-resolution Hall sensor, regenerative braking, plug braking, six-step commutation braking

1 Introduction

With the challenges of energy and environment crisis, new-energy vehicles have been the focus of the automotive industry. Battery electric vehicles have the advantages of high efficiency and zero emission and have been developed intensively by automotive manufacturers. Limited by the battery technology, battery electric vehicles are still not competitive enough compared with conventional vehicles in the aspects of driving range and cost. Micro electric vehicle is less battery critical and should be given priority in research as the first step into the electric driving era.

"Micro-Harry" is an experimental micro electric vehicle, which is driven by four in-wheel permanent magnetic synchronous motor (PMSM)[1], as shown in Fig. 1.

PMSM is widely used as traction motor in electric vehicles with the advantages of high power density and high efficiency[2–3]. FOC is appropriate for PMSM with sinusoidal back-EMF and has been researched intensively[4–5]. Recently, sensorless control of PMSM has been highlighted[6–7] in order to improve the reliability and cut the cost of high-resolution rotor position sensors, such as resolvers. However, while sensorless control can identify rotor position with enough accuracy at high speed range, the low speed performance could not meet the requirement of electric vehicles.

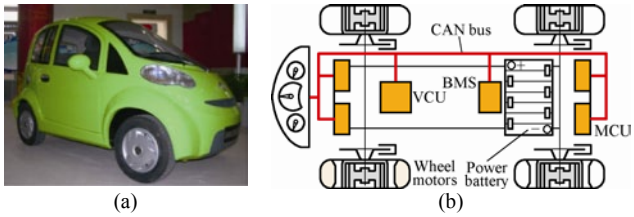

(a) (b)

Fig. 1. "Micro-Harry" electric vehicle driven by four in-wheel motors

The rotor position of the in-wheel PMSM in "Micro-Harry" is acquired by three low-resolution Hall

* Corresponding author. E-mail: ouymg@tsinghua.edu.cn
This project is supported by National Hi-tech Research and Development Program of China (863 Program, Grant No. 2008AA11A126), and Program for New Century Excellent Talents in University of China (Grant No. NCET-10-0498)

sensors. Typically simple six-step commutation control is applied, but the high torque ripple and thus the noise and vibration problems are big drawbacks of the six-step commutation control. This paper tries to improve the performance using FOC based on low-resolution Hall sensors.

Regenerative braking is a great advantage of electric vehicles over conventional vehicles. Kinetic energy can be recovered to energy storage devices instead of being wasted as heat. So regenerative braking is a key technology to extend the driving range, which is limited by the on-board battery capacity. Regenerative braking can be realized by six-step commutation control[8–9] and FOC[10–11]. At low speed range where no enough braking torque could be delivered by regenerative braking, plug braking is necessary, but energy is drawn out of the battery instead of being recovered in plug braking.

This paper firstly illustrates the FOC of PMSM with low-resolution Hall-effect sensors. Then the braking control algorithms based on six-step commutation and FOC are discussed in details. The driving and braking control is verified by tests on dynamometer. Summary and conclusion are drawn finally.

2 FOC Driving Control of PMSM Based on Hall Sensors

2.1 FOC of PMSM

"Micro-Harry" adopts non-salient outer rotor PMSMs. Fig. 2 shows the sketch of the control circuit. The electrical model of PMSM in the d-q reference frame can be expressed as in Eqs. (1) and (2):

$$\begin{pmatrix} u_\mathrm{d} \\ u_\mathrm{q} \end{pmatrix} = \begin{pmatrix} R_\mathrm{s} + pL_\mathrm{d} & -\omega L_\mathrm{q} \\ \omega L_\mathrm{d} & R_\mathrm{s} + pL_\mathrm{q} \end{pmatrix} \begin{pmatrix} i_\mathrm{d} \\ i_\mathrm{q} \end{pmatrix} + \begin{pmatrix} 0 \\ \omega \psi_\mathrm{f} \end{pmatrix}, \tag{1}$$

$$T_\mathrm{em} = n_\mathrm{p} \psi_\mathrm{f} i_\mathrm{q}, \tag{2}$$

where u_d, u_q—d- and q-axis terminal voltages,
i_d, i_q—d- and q-axis armature currents,
L_d, L_q—d- and q-axis inductances,
R_s—Armature resistance,
ω—Electrical angular velocity,
ψ_f—Permanent magnet flux-linkage,
n_p—Number of pole pairs,
p—Differential operator, p=d/dt.

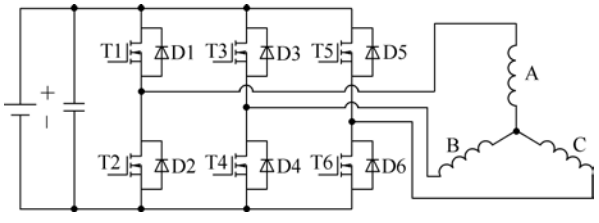

Fig. 2. Sketch of the control circuit of PMSM

L_d and L_q are equal for non-salient motors. As indicated by Eq. (2), the motor torque is determined only by i_q and has nothing to do with i_d. In order to get a better motor efficiency, i_d is controlled to be zero during operation to reduce the copper loss. The control diagram of FOC is illustrated in Fig. 3. The precision of position estimation is crucial for FOC performance.

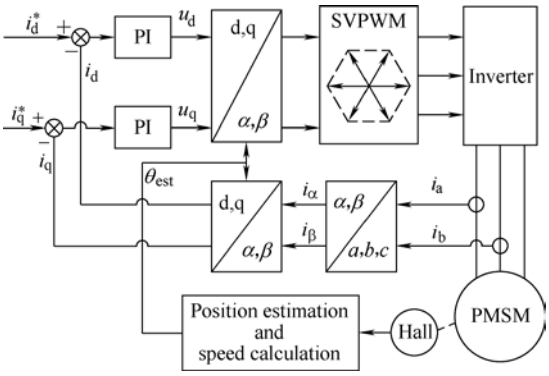

Fig. 3. Control diagram of FOC for PMSM

2.2 Position estimation based on Hall sensors

2.2.1 Position estimation algorithm

Three Hall sensors are employed for rotor positioning, as shown in Fig. 4. The combination of three Hall sensors divides an electrical cycle into 6 intervals as shown in Fig. 5, which means that only an accuracy of 60 electrical degrees could be achieved. In order to get a continuous and precise rotor position signal, Hall signals need to be further processed.

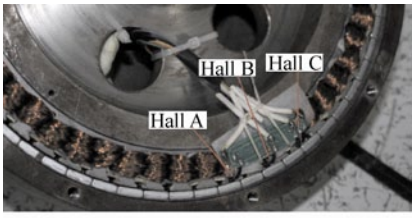

(a)

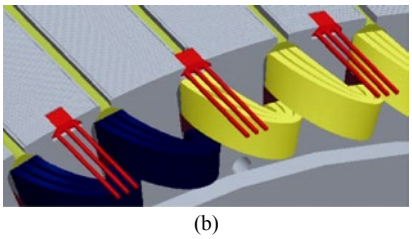

(b)

Fig. 4. Hall sensors in PMSM

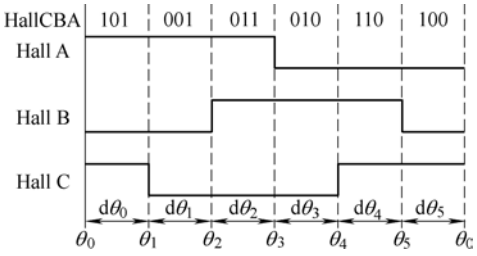

Fig. 5. Hall signals during an electrical cycle

The basic idea of improving the positioning accuracy is to do interpolation between two consecutive Hall signals using the estimated motor speed, which can be illustrated by Fig. 6[12]. Hall signals update the rotor position every 60 electrical degrees as at t_0 and t_1, which correspond to the rotor positions of θ_0 and θ_1. The position difference between θ_0 and θ_1 is 60 electrical degrees. The average motor speed ω_{est} between t_0 and t_1 could be calculated using Eq. (3):

$$\omega_{est} = \frac{\pi/3}{t_1 - t_0}. \tag{3}$$

Then the position at instant of time t is approximated as in Eq. (4):

$$\theta_{est} = \theta_1 + \omega_{est}(t - t_1). \tag{4}$$

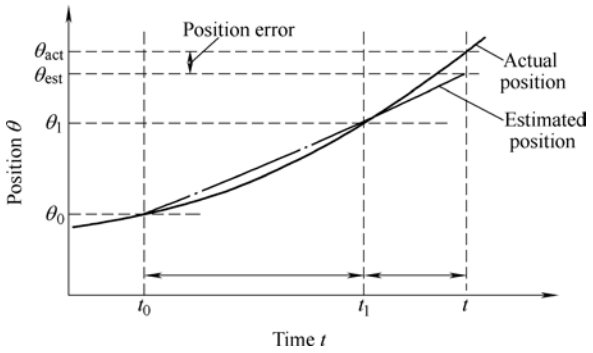

Fig. 6. Position estimation based on Hall sensors

The position estimation method is based on the assumption that the motor speed is kept constant, which is not realistic in vehicle operations, especially when the vehicle is running in a rapid accelerating or a hard braking condition. As in Fig. 6 when the motor is accelerating, the estimated motor speed is the average speed in the last Hall interval, so it's smaller than the actual motor speed and the position error comes out.

Methods to compensate for the motor dynamics are proposed in Refs. [12–13]. Ref. [12] suggests to compensate the estimated position with the motor acceleration according to the estimated motor torque. But this only works if the load torque is relatively stable or at least predictable, which is typical for industry applications but not likely to happen in vehicle operations. For example, the acceleration of a vehicle running uphill may be quite different with that of a vehicle running downhill with the same driving torque. A forecast algorithm is proposed in Ref. [13] taking the motor acceleration into consideration, which is calculated based on the average motor speeds in the past two Hall intervals. However, the acceleration is quite unpredictable in complicated operation situations, especially in low speed range. When the acceleration changes suddenly, the estimated acceleration cannot follow the actual value quickly enough. In this case, the compensation method might reversely impair the positioning accuracy. Methods to improve the positioning accuracy, which are suitable for vehicle application in complicated situations, remain for further research.

2.2.2 Compensation for misalignment of Hall sensors

Ideally, the Hall sensors are located with 120 electrical degrees apart, and each Hall interval corresponds to 60 electrical degrees. But in real applications, the position error caused by the misalignment of Hall sensors cannot be neglected. As shown in Fig. 4, the Hall sensors are placed in the stator coils. With a stator diameter of 198 mm and 46 poles rotor, a misalignment of 0.5 mm of the Hall sensor could lead to a position error of 6.7 electrical degrees.

As shown in Fig. 7, the misalignment of Hall sensors can cause an uneven distribution of Hall intervals, which needs to be compensated.

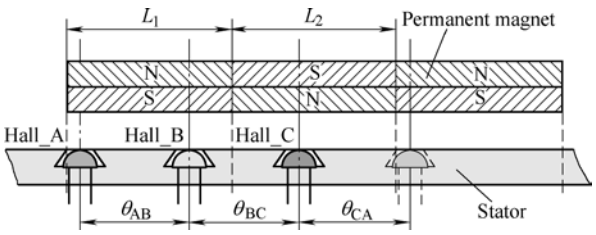

Fig. 7. Misalignment of Hall sensors

To measure the actual distribution of Hall intervals, the motor is driven by the dynamometer at a constant speed, and then the position intervals are proportional to the time intervals between Hall transitions. As can be seen from the experiment result shown in Fig. 8, the actual Hall intervals deviate a lot from the ideal value of 60 electrical degrees, and the maximum position error of the measured motor is over 8 electrical degrees, which could have much influence on the control performance. As a result, the motor speed estimation in Eq. (3) should be modified as in Eq. (5):

$$\omega_{est} = \frac{\theta_1 - \theta_0}{t_1 - t_0}. \tag{5}$$

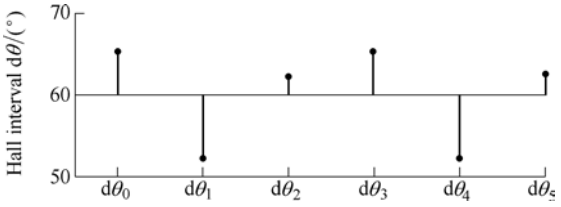

Fig. 8. Hall intervals measured at a constant motor speed

3 Electrical Braking Control of PMSM

Both regenerative braking and plug braking can be applied to decelerate a PMSM. But kinetic energy is transformed into electric energy and restored in batteries in regenerative braking, while electric energy is drawn out of batteries to generate braking torques in plug braking.

Although the motor is characterized with a sinusoidal

back EMF, braking control methods based on six-step commutation derived from motors with trapezoidal back EMF can still be applied and satisfactory braking performances can be achieved. A more accurate control of braking torque can be realized in d-q axis frame as in FOC.

3.1 Six-step commutation electrical braking control

3.1.1 Six-step commutation regenerative braking

For permanent magnetic motors powered by batteries, the back EMF is smaller than the battery voltage, so the boost converter circuit is necessary to guide the current back to the battery. The principle of the boost circuit is explained in Ref. [15], so it's not going to be detailed here.

Generally, there are two variants of six-step commutation braking, namely half-bridge commutation braking and full-bridge commutation braking, whose principles are explained in Fig. 9. The upmost three curves are the back EMFs of Phase A, B and C represented by the red, green and blue curves respectively. Then the control signals of the inverter. High-bridge commutation and low-bridge commutation, as two variants of half-bridge commutation are basically equivalent to each other, so only high-bridge commutation is shown here.

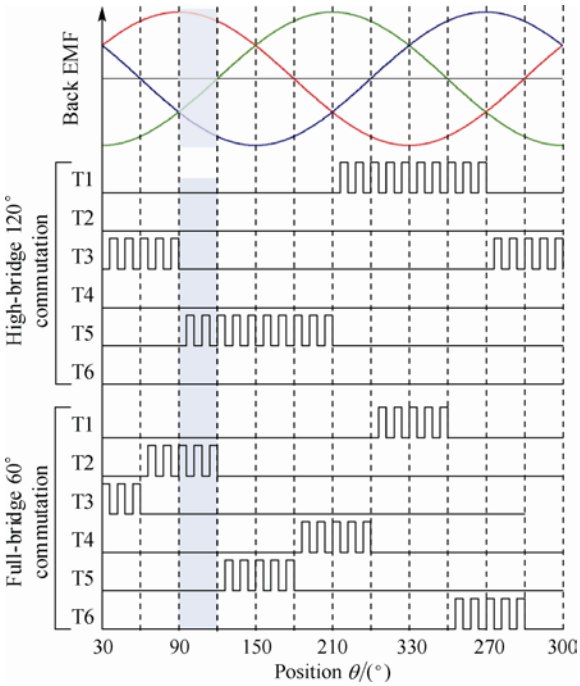

Fig. 9. Regenerative braking based on six-step commutation

As can be seen from Fig. 9, each high-bridge is ON for 120 electrical degrees and low-bridge is kept OFF in one electrical cycle in high-bridge commutation braking, while each bridge is ON for 60 electrical degrees in full-bridge commutation braking. As a result, the load unbalance between high-bridge and low-bridge may be a problem for half-bridge commutation braking if the motor is kept in the regenerative braking mode for a long time.

Compared with the half-bridge commutation braking, full-bridge commutation braking can better explore the potential of the back EMF of the motor. Take the shadowed interval (90°–120°) in Fig. 9 for example. Fig. 10 and Fig. 11 show the states in high-bridge commutation braking and full-bridge commutation braking respectively. One significant difference between the two control strategies is that, in high-bridge commutation mode the back EMF of Phase B is reversely blocked and thus does not contribute to electrical braking, while full-bridge commutation braking can make full use of the back EMFs of all three phases.

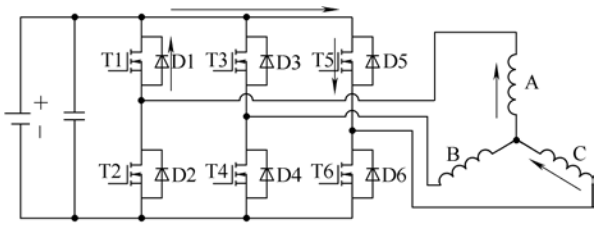

(a) T5 is ON

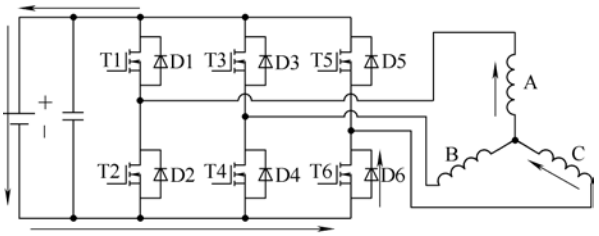

(b) T5 is OFF

Fig. 10. High-bridge commutation braking

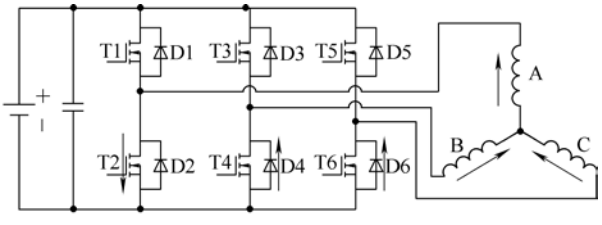

(a) T2 is ON

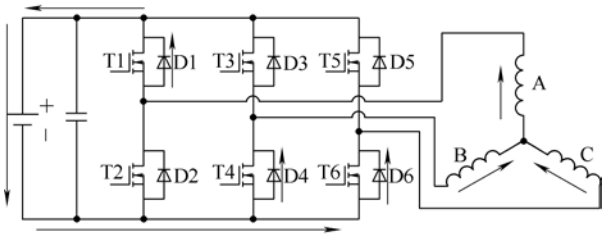

(b) T2 is OFF

Fig. 11. Full-bridge commutation braking

3.1.2 Six-step commutation plug braking

Plug braking is to drive the motor in the reverse direction. The electric power from the batteries and the back EMF of the motor generate a braking torque to decelerate the vehicle. Electric energy and kinetic energy are transformed into heat in the motor.

Fig. 12 shows the ON/OFF states of the six half-bridges

in normal driving and plug braking. Apparently, the ON/OFF states in plug braking are just opposite to those in normal driving.

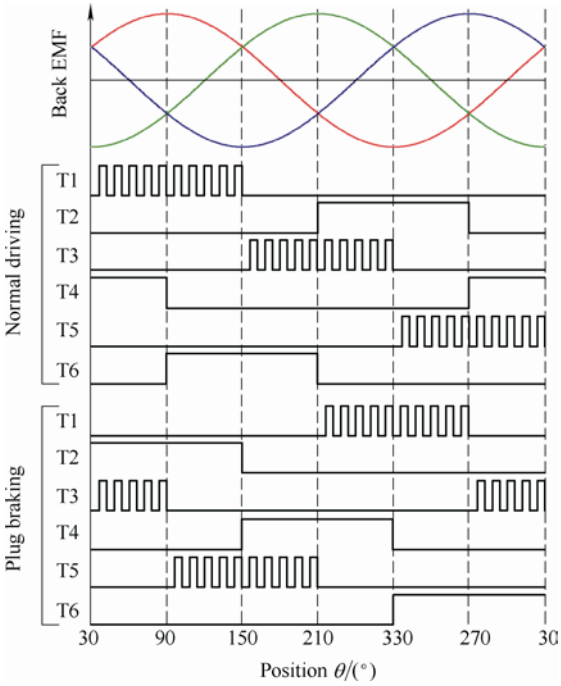

Fig. 12. Normal driving and plug braking based on six-step commutation

3.2 FOC electrical braking control

As shown in Eq. (2), the motor torque is proportional to i_q, so a braking torque can be generated by requesting a negative i_q in FOC. Considering a steady operating state and i_d being zero, Eq. (1) can be rewritten as Eq. (6):

$$\begin{cases} u_d = -\omega L_q i_q, \\ u_q = R_s i_q + \omega \psi_f. \end{cases} \tag{6}$$

Fig. 13 shows the phasor diagram of the PMSM in FOC. Figs. 13(a), 13(b) and 13(c) correspond to normal driving, regenerative braking and plug braking modes respectively. The motor electromagnetic power P_{em} and the stator input power P_{in} can be expressed as in Eq. (7). A positive P_{em} corresponds to the driving mode, while a negative P_{em} corresponds to the braking mode. A positive P_{in} means that electric power is drawn out of the battery, while a negative P_{in} means that electric power is regenerated into the battery:

$$\begin{cases} P_{em} = \dfrac{EU \sin\theta}{X_q}, \\ P_{in} = U i_q \cos\varphi, \end{cases} \tag{7}$$

where X_q—Reactance in q-axis,
E—Back EMF,
U—Stator voltage,
θ—Load angle,
φ—Phase angle.

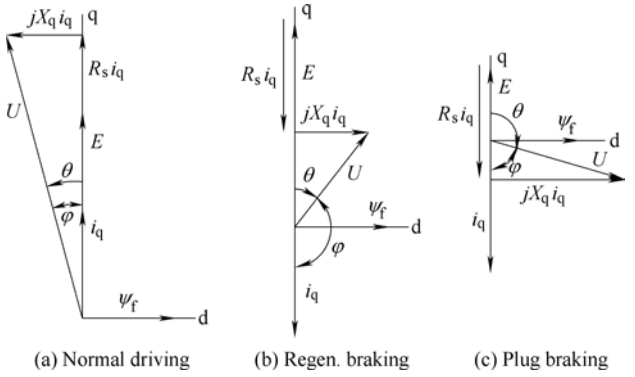

(a) Normal driving (b) Regen. braking (c) Plug braking

Fig. 13. Phasor diagram of PMSM in FOC

In normal driving mode, U leads E by phase θ and the load angle θ is equal to the phase angle φ. This operating mode can be characterized by Eq. (8). Electric power is drawn out of the battery. Most of the power is transformed into electromagnetic power and some of it is transformed into losses (mainly copper loss in the stator winding).

$$\begin{cases} 0 < \theta < \dfrac{\pi}{2}, 0 < \varphi < \dfrac{\pi}{2}, \\ P_{em} > 0, P_{in} > 0. \end{cases} \tag{8}$$

3.2.1 FOC regenerative braking

Fig. 13(b) is the phasor diagram in regenerative braking mode. u_d is in the opposite phase as in normal driving mode due to the negative i_q, while u_q is still in the same phase as in normal driving mode. As a result, U lags behind E by phase θ, and the phase angle φ is larger than $\pi/2$, so P_{in} and P_{em} both are negative, as expressed in Eq. (9). This means electromagnetic power is trying to decelerate the motor and electric power is drawn into the battery.

$$\begin{cases} -\dfrac{\pi}{2} < \theta < 0, \dfrac{\pi}{2} < \varphi < \pi, \\ P_{em} < 0, P_{in} < 0. \end{cases} \tag{9}$$

Neglecting the mechanical loss, the mechanical braking power is equal to the electromagnetic power and the braking torque is equal to the electromagnetic torque. Then how the stator input power and the braking power change with the braking torque needs to be discussed. Since the braking torque is proportional to i_q, braking torque is represented by i_q in the following discussion.

Eq. (7) can be rewritten as Eq. (10) according to the geometric relationship of the phasor diagram:

$$\begin{cases} P_{em} = \psi_f i_q \omega, \\ P_{in} = (\omega \psi_f + R_s i_q) i_q. \end{cases} \tag{10}$$

As indicated by Eq. (10), at a given motor speed the braking power is proportional to the braking torque, while

the regeneration power is a quadratic function of the braking torque as shown in Fig. 14.

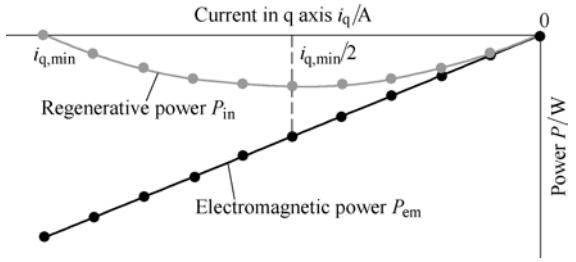

Fig. 14. Regenerative power and electromagnetic power changes with i_q

With the increase of braking torque, i_q becomes smaller (i_q is negative) and phase angle φ decreases. As long as φ is larger than $\pi/2$, P_{in} stays negative, which means that energy is restored in the battery. In order to stay in the regeneration braking mode, there is a minimum limit for i_q where u_q decreases to zero, so the minimum i_q can be expressed in Eq. (11):

$$i_{q,\min} = -\frac{\omega \psi_f}{R_s}. \tag{11}$$

When maximum braking torque is generated, no electric energy is recovered, and all the kinetic energy is transformed into heat in the stator winding. Since the regenerative power is a quadratic function of i_q, the maximum regenerative power is achieved at half of the maximum braking torque.

At high speed, this minimum i_q as in Eq. (11) could be neglected because of the limits of motor torque capacity and inverter power capacity. As shown in Fig. 15, the maximum braking torque is increases with the motor speed and it's so large at high speed that it already goes beyond the inverter capacity, so this limit only needs to be taken into consideration at low speed. Attention should be paid when braking at low speed in order to stay in the regenerative braking zone. The braking torque where the most electric power could be recovered into the battery is also shown in Fig. 15.

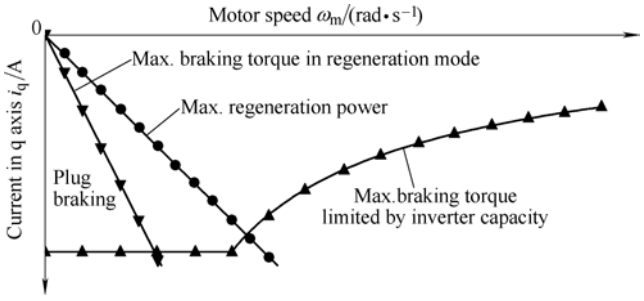

Fig. 15. Limits of regenerative braking torque

3.2.2 FOC plug braking

At low speed, if a high braking torque is demanded, u_q may be in the reverse phase, which makes the phase angle φ less than $\pi/2$, as shown in Fig. 13(c). This means that the back EMF is not enough to generate the required braking torque and electric power is drawn out of the battery to assist the back EMF. Plug braking is also shown in Fig. 15 as the area below the red curve.

Plug braking mode can be characterized as in Eq. (12):

$$\begin{cases} -\pi < \theta < \dfrac{\pi}{2}, 0 < \varphi < \dfrac{\pi}{2}, \\ P_{em} < 0, P_{in} > 0. \end{cases} \tag{12}$$

4 Experiment Results

The driving and braking control algorithms of PMSM are studied in experiments. The experiments are mainly carried out at the test bench where the dynamometer could function as a load to the motor or drive the motor when the motor is in braking mode.

4.1 FOC driving control

Fig. 16 shows the signals in a FOC startup process. As can be seen that, i_q follows the target value very well and i_d is controlled to be near zero. Attention should be paid to the first electrical cycle of the startup where the rotor position value shows a step-climbing curve. As discussed in Fig. 6, during the accelerating process, the estimated speed lags behind the actual value, therefore the interpolated rotor position between Hall transitions cannot be well estimated. But both in dynamometer tests and vehicle tests, this position error proves to be not a big problem. Satisfactory performance can be achieved with this position estimation algorithm. It would be nice of course if the positioning accuracy could be further improved by some algorithm especially during the startup process.

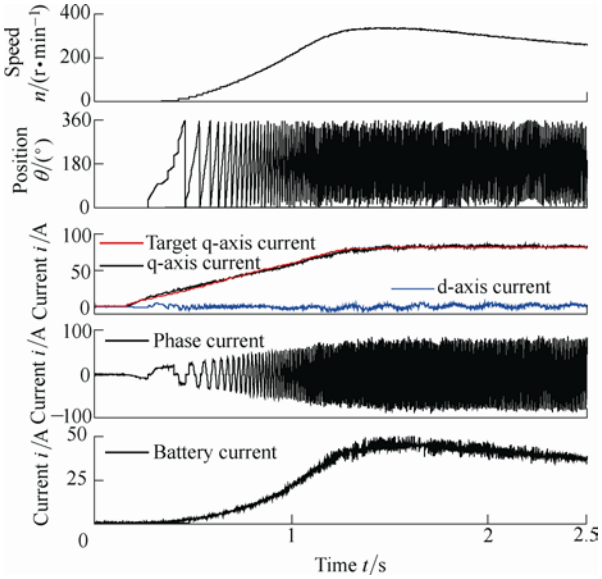

Fig. 16. Startup of PMSM in FOC

4.2 Braking control

Braking control algorithms based on six-step

commutation and FOC are studied and compared in experiments in this section. The current signal is converted into voltage signals using a Hall current sensor and a sampling resistor, and then sent to the oscilloscope. A voltage of 1 V across the resistor corresponds to a current of 40 A.

4.2.1 Six-step commutation regenerative braking

The plug braking can be considered as six-step driving in the opposite direction and is not going to be discussed here. Only regenerative braking based on six-step commutation is presented in this section.

The high-bridge commutation control is studied at first. Fig. 17 shows the phase current and battery current when the motor is running at 150 r/min and the duty cycle is set to be 64%. The blue curve and the purple curve represent the phase current and the battery current respectively. The slight positive value of the battery current is due to the static error of the oscilloscope. In this condition, no continuous phase current could be observed and the battery current is almost zero. A slight braking torque of 2.4 N • m is generated. In Fig. 18, the motor speed rises to 350 r/min and the duty cycle is kept unchanged. A braking torque of 39.8 N • m and a regenerative current of 21.5 A are generated.

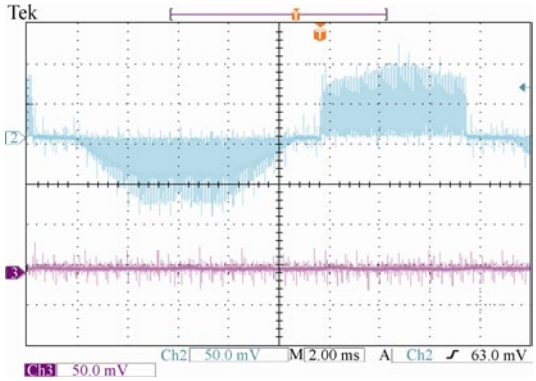

Fig. 17. Regenerative braking control of high-bridge commutation at 150 r/min

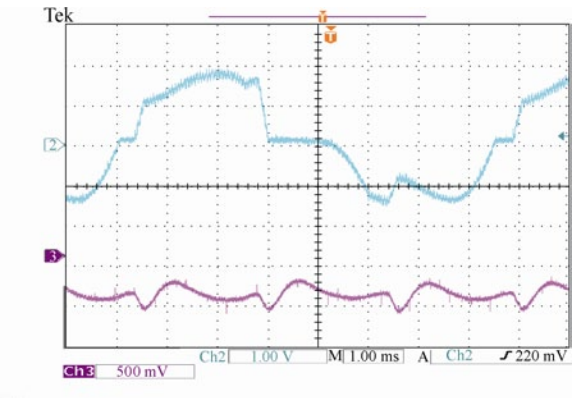

Fig. 18. Regenerative braking control of high-bridge commutation at 350 r/min

Fig. 19 and Fig. 20 show the results of full-bridge commutation braking control in the same operating condition as in the high-bridge commutation braking. No continuous phase current can be observed and the battery current is almost zero at the speed of 150 r/min, and the braking torque is 2.4 N • m, which is also the same as in the high-bridge commutation braking. When the speed rises to 350 r/min, a braking torque of 43.1 N • m and a regenerative current of 23.5 A are generated.

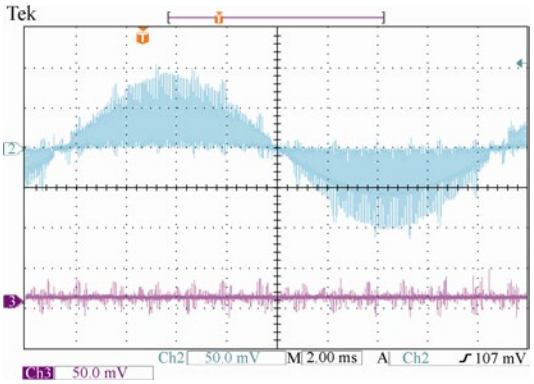

Fig. 19. Regenerative braking control of full-bridge commutation at 150 r/min

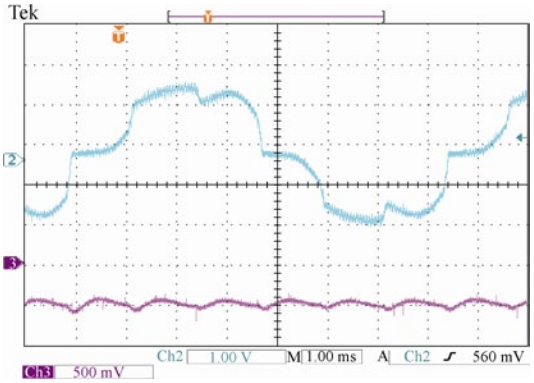

Fig. 20. Regenerative braking control of full-bridge commutation at 350 r/min

Significant differences of the current shape between these two braking methods can be observed. In the high-bridge braking, the phase current is asymmetric. The positive current lasts for only 120 electrical degrees when the high bridge is ON, while the negative current lasts for almost 180 electrical degrees. In the full-bridge braking, the positive and negative currents both last for about 150 electrical degrees. The phase current distribution of the full-bridge braking is more “even” compared to the high-bridge braking, and the battery current ripple is also smaller.

4.2.2 FOC regenerative braking control

FOC braking control is realized by requesting a negative i_q corresponds to the braking torque demand. For comparison, the operating conditions are set to be close to the six-step commutation braking.

Fig. 21 shows the phase current and battery current at the speed of 150 r/min and the braking torque is 2.4 N • m. Similarly, the phase current is not continuous and almost no regenerative current is available. The phase current shape is

quite similar to Fig. 19.

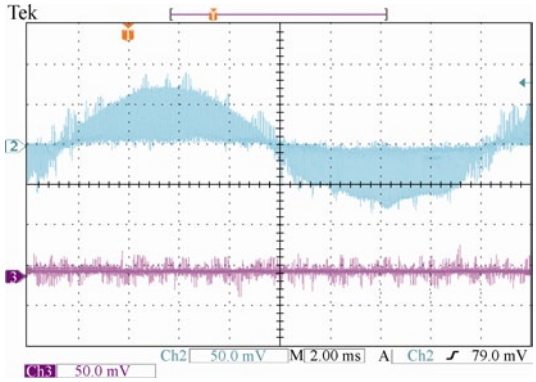

Fig. 21. Regenerative braking control of FOC at 150 r/min

Fig. 22 shows the currents at the speed of 350 r/min and the braking torque is 43.4 N • m. A regenerative current of 25.2 A is generated. The phase current shows a very good sinusoidal shape, and the battery current ripple is even smaller than full-bridge braking.

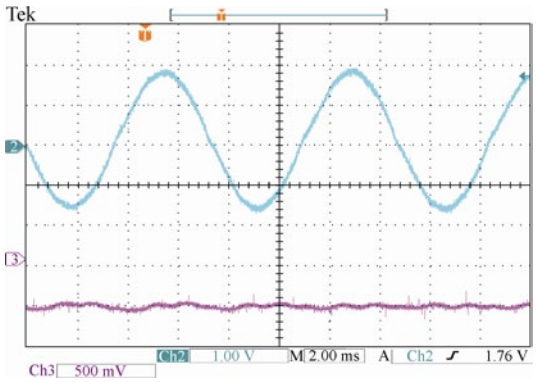

Fig. 22. Regenerative braking control of FOC at 350 r/min

4.2.3 Comparison of regenerative braking algorithms

A brief comparison between these three regenerative braking algorithms is made at the same operating point as in Table 1.

Table 1. Comparison of regenerative braking

Braking algorithm	Motor speed n/(r • min^{-1})	Braking torque T/(N • m)	Battery voltage U_{bat}/V	Battery current I_{dc}/A	Efficiency η/%
High-bridge commutation	350	39.8	51.85	21.5	76.42
Full-bridge commutation	350	43.1	51.90	23.5	77.21
FOC	350	43.4	51.95	25.2	82.30

As can be seen from Table 1, FOC braking shows the best efficiency, while half-bridge is the worst. At the same motor speed and the same duty cycle, full-bridge braking can better explore the potential of the back EMFs and thus higher braking torque and higher efficiency are achieved, as discussed in section 3.1.1. A smooth regenerative current is realized by FOC braking, while the battery current ripple of half-bridge braking is the largest. Limited by the accuracy and band width of the torque sensor, the braking torque ripple cannot be measured, but it's quite sure that torque ripple performance of FOC braking is the best and half-bridge braking is the worst, because the torque ripple can be indicated by the vibration and noise of the test bench.

Another advantage of FOC braking is that the transition between regenerative braking mode and plug braking mode can be very smooth, as would be shown in the next section. From the above discussion, the decision is made to choose FOC braking as the braking algorithm for its advantages over six-step commutation braking.

4.2.4 Regenerative braking and plug braking of FOC

As discussed in section 3.2, the motor is running in regenerative braking mode when the braking torque is small. With the increase of braking torque, u_q keeps decreasing. If u_q turns negative, the motor is working in the plug braking mode. This mode transition is illustrated by Fig. 23. The motor is running at a constant speed of 150 r/min. With the increase of the braking torque (i_q decreases), the regenerative current firstly increases (battery current decreases) and then decrease back to zero. When the braking torque keeps increasing, the battery current goes positive, which means that the motor has turned from regenerative braking mode into plug braking mode. The curve shape of the battery current is analog to the regenerative power curve in Fig. 14.

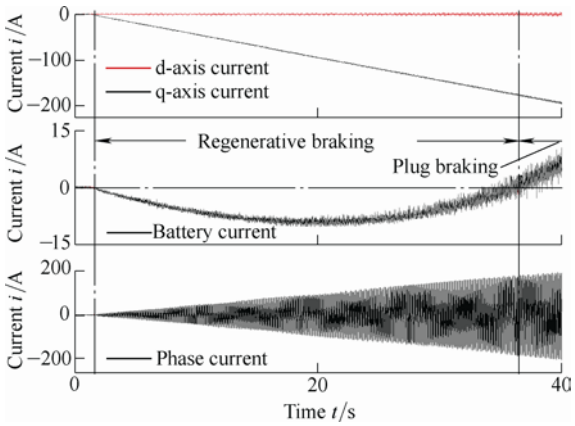

Fig. 23. Braking control of FOC at 150 r/min

In plug braking mode, the battery supplies power to the motor to generate the required braking torque together with the back EMFs. So the motor should avoid working in the plug braking mode if not urgently necessary. The vehicle control unit (VCU) should know the limit of regenerative braking and the maximum regenerative power at each operating point in order to make the right decision.

5 Conclusions

(1) FOC algorithm is developed for PMSM based on low-resolution Hall-effect sensors. The positioning

accuracy of the Hall sensors is improved by interpolation between two consecutive Hall signals using the estimated motor speed.

(2) The positioning error from the misalignment of the Hall sensors is compensated by the precise calibration of Hall transition timing, which is crucial for the driving and braking control of the motor.

(3) Two variants of the six-step commutation braking control are discussed in details. The full-bridge braking can better explore the potential of the back EMFs, thus can deliver higher efficiency and smaller current ripple than half-bridge braking.

(4) The FOC braking is realized by requesting a negative i_q according to the braking torque demand. The best efficiency and the smallest current ripple are achieved with FOC braking, compared with six-step commutation braking. As a result, FOC braking is chosen as the braking control algorithm for electric vehicles.

(5) The FOC regenerative braking and plug braking are analyzed by using phasor diagrams. At a given motor speed, the motor can only stay in the regenerative zone if the braking torque doesn't exceed a certain limit, which is proportional to the motor speed. If the braking torque exceeds this limit, the motor turns into plug braking mode. The braking torque at which the maximum regenerative power is generated is half of this limit.

(6) The driving and braking control of PMSM is studied in experiments. The experiment results verify that the control algorithms can achieve good performances.

References

[1] MA Yan, ZHANG Kangkang, GU Jing, et al. Design of the control system for a four-wheel driven micro electric vehicle[C]// *Proceedings of 5th IEEE Vehicle Power and Propulsion Conference, VPPC '09*, Dearborn, MI, USA, September 7–10, 2009: 1 813–1 816.

[2] CHAU K T, CHAN C C, LIU Chunhua. Overview of permanent-magnet brushless drives for electric and hybrid electric vehicles[J]. *IEEE Transactions on Industrial Electronics*, 2008, 55(6): 2 246–2 257.

[3] TERASHIMA M, ASHIKAGA T, MIZUNO T, et al. Novel motors and controllers for high-performance electric vehicle with four in-wheel motors[J]. *IEEE Transactions on Industrial Electronics*, 1997, 44(1): 28–38.

[4] PARK J W, KOO D H, KIM J M, et al. Improvement of control characteristics of interior permanent-magnet synchronous motor for electric vehicle[J]. *IEEE Transactions on Industry Applications*, 2001, 37(6): 1 754–1 760.

[5] BAIK I C, KIM K H, YOUN M J. Robust nonlinear speed control of PM synchronous motor using adaptive and sliding mode control techniques[J]. *IEE Proceedings of Electric Power Applications*, 1998, 145(4): 369–376.

[6] JOHNSON J P, EHSANI M, GUZELGUNLER Y. Review of sensorless methods for brushless DC[C]// *Proceedings of 1999 Industry Applications Conference, Thirty-Fourth IAS Annual Meeting*, Phoenix, USA, October 3–7, 1999(1): 143–150.

[7] ICHIKAWA S, TOMITA M, DOKI S, et al. Sensorless control of permanent-magnet synchronous motors using online parameter identification based on system identification theory[J]. *IEEE Transactions on Industrial Electronics*, 2006, 53(2): 363–372.

[8] HUANG Feili, JIANG Xinjian, WANG Yaoming. A dedicated permanent magnet synchronous motor drive system for electric vehicle[C]//*Proceedings of 26th Annual IEEE Power Electronics Specialists Conference, PESC '95*, Atlanta, USA, June 18–22, 1995(1): 252–257.

[9] BECERRA R C, EHSANI M, JAHNS T M. Four-quadrant brushless ECM drive with integrated current regulation[J]. *IEEE Transactions on Industry Applications*, 1992, 28(4): 833–841.

[10] CHEN Rong, DENG Zhiquan, YAN Yangguang. Analysis of braking process of permanent magnet synchronous motor based on rotor field-oriented control[J]. *Transactions of China Electrotechnical Society*, 2004, 19(9): 30–36. (in Chinese)

[11] JIE Guisheng, MA Weiming. Research on the braking of the permanent magnet synchronous motor drives for electric vehicle[J]. *Journal of Wuhan University of Technology (Transportation Science and Engineering)*, 2007, 31(1): 133–136. (in Chinese)

[12] MORIMOTO S, SANADA M, TAKEDA Y. High-performance current-sensorless drive for PMSM and SynRM with only low-resolution position sensor[J]. *IEEE Transactions on Industry Applications*, 2003, 39(3): 792–801.

[13] LU Dongbin, GU Jing, LI Jianqiu, et al. High-performance control of PMSM based on a new forecast algorithm with only low-resolution position sensor[C]//*Proceedings of 5th IEEE Vehicle Power and Propulsion Conference, VPPC '09*, Dearborn, MI, USA, September 7–10, 2009: 1 440–1 444.

[14] SUN Lizhi, LU Yongping, DENG Zhaochun. Analysis and Simulation of Regenerative Braking of PM Synchronous Motors[J]. *Small and Special Electrical Machines*, 1997, 6: 8–10. (in Chinese)

[15] CHEN Tien-Chi, REN Tsai-Jiun, CHEN Yi-Shuo, et al. Driving and regenerative braking method for energy-saving wheel motor[C]// *Proceedings of SICE Annual Conference 2010*, Taipei, China, August 18–21, 2010: 2 654–2 659.

Biographical notes

GU Jing, born in 1985, is currently a PhD candidate at *State Key Laboratory of Automotive Safety and Energy, Tsinghua University, China*. He received his bachelor degree in Automotive Engineering from *Tsinghua University, China*, in 2006. His research interests include powertrain control of electric vehicles.
Tel: +86-10-62785706; E-mail: gu-j02@mails.tsinghua.edu.cn

OUYANG Minggao, born in 1958, is currently a professor at *Department of Automotive Engineering, Tsinghua University, China*. He received his PhD degree in mechanical engineering from *the Technical University of Denmark, Lyngby*, in 1993. His research interests include new energy vehicles, automotive powertrains, engine control systems, and transportation energy strategy and policy.
E-mail: ouymg@tsinghua.edu.cn

LI Jianqiu, born in 1972, is currently a professor at *Department of Automotive Engineering, Tsinghua University, China*. He received his PhD degree in power mechanism and engineering from *Tsinghua University, China*, in 2000. His research interests include electronic control of diesel engine, key technology of automotive electronics, fuel cell and powertrain control.
E-mail: lijianqiu@tsinghua.edu.cn

LU Dongbin, born in 1982, is currently a PhD candidate at *State Key Laboratory of Automotive Safety and Energy, Tsinghua University, China*. He received his bachelor degree in electrical engineering from *Shandong University, China*, in 2006 and M.S. degree in electrical and electronic engineering from *Huazhong University of Science and Technology, China*, in 2008. His research interests are modeling, design and control of the powertrain system for a hybrid electric vehicle.

E-mail: ldb08@mails.tsinghua.edu.cn

FANG Chuan, born in 1990, is currently a PhD candidate at *State Key Laboratory of Automotive Safety and Energy, Tsinghua University, China*. He received his bachelor degree in Automotive Engineering from *Tsinghua University, China*, in 2010. His research interests include powertrain control of electric vehicles.
E-mail: fangchuan1990@126.com

MA Yan, born in 1986, received her master degree in power mechanism and engineering from *Tsinghua University, China*, in 2010. Her research interests include regenerative braking of electric vehicles.
E-mail: eleanor.mayan@gmail.com